Nigerian Journal of Physics (NJP)
ISSN online: 3027-0936
ISSN print: 1595-0611
DOI: https://doi.org/10.62292/njp.v35i(S).2026.741
Volume 35(S), November 2026

Thermal Annealing Effects on the Optical, Electrical, and Surface Characteristics of Electrodeposited Aluminium-Doped TiO□ Thin Films

***[1]Kazeem A. Musiliyu, [2]Enoch D. Ogunmola, [1]Abiodun E. Adeoye, [2]Olumuyiwa A. Alao, [2]Akintunde A. Ajayi, [1]Luqman E. Oloore**

[1]Department of Physics and SLT, Abiola Ajimobi Technical University, Ibadan, Nigeria
[2]Afe Babalola University, Ado Ekiti, Nigeria

*Corresponding Author's Email: kazeem.musiliyu@tech-u.edu.ng

Keywords:
Aluminium doping;
Annealing temperature;
Electrodeposition;
Tio_2 thin films;
Optical band gap;
Electrical conductivity

Submitted: 22/09/2026

Accepted: 7/11/2026

Published: 9/11/2026

ABSTRACT

The thermal response of aluminium-doped titanium dioxide (Al:TiO_2) thin films is important for tailoring their optical and electrical properties for functional applications. In this study, Al:TiO_2 thin films were electrodeposited on indium tin oxide (ITO) glass substrates under constant precursor and deposition conditions and annealed at 200, 300, 400, 500, 600, and 700 °C for 60 min. The nominal Al concentration and deposition parameters were maintained constant to isolate the effect of annealing temperature. Optical properties were evaluated using UV–visible spectroscopy, electrical conductivity by the four-point-probe technique, and surface morphology by scanning electron microscopy (SEM). The films exhibited high visible-light transmittance, generally exceeding 80%, with values of approximately 91–93% between 450 and 800 nm. The apparent optical band gap decreased from 3.00 eV at 200 °C to 2.85 eV at 700 °C, accompanied by a red shift in the absorption edge. Electrical conductivity increased from 1.263 S cm^{-1} at 200 °C to 3.609 S cm^{-1} at 700 °C, while resistivity decreased from 0.792 to 0.277 Ω cm. SEM revealed temperature-dependent changes in particle development, interparticle contact, and surface organization. These results demonstrate that post-deposition annealing effectively regulates the optical, electrical, and morphological characteristics of electrodeposited Al:TiO_2 films. The combination of high optical transmission and enhanced conductivity supports their potential for transparent optoelectronic, sensing, photoelectrochemical, and photovoltaic-related structures. Complimentary structural, chemical, and device-level studies are required to clarify the mechanisms underlying these changes and establish practical device performance.

INTRODUCTION

The properties of oxide thin films depend on the complex interactions among composition, microstructure, surface characteristics, and processing history (Wang et al., 2020). This interdependence is particularly relevant for coatings engineered to achieve high optical transmission and suitable electrical transport. Irrespective of the specific deposition process, post-deposition heat treatment can significantly alter the resulting state of a thin film and is therefore a critical processing parameter. Electrodeposition provides an attractive route for oxide-film growth owing to the relative simplicity of electrochemical deposition directly onto electrically conductive substrates (Kumar et al., 2024; Musiliyu et al., 2023; Kalinina and Elena, 2021). By appropriately selecting the electrodeposition parameters, nucleation sites, particle size, film integrity, and surface morphology can be tailored. Nevertheless, the properties of as-deposited films can evolve significantly during subsequent heating, making annealing temperature an important processing parameter. TiO_2 is a promising oxide semiconductor for applications in sensing, photoelectrochemical, photovoltaic, and optoelectronic devices owing to its chemical stability, optical properties, photocatalytic activity, and sensing capabilities (Taneja et al., 2024). The properties of TiO_2 thin films are closely related to their crystalline phase, crystallite size, defect characteristics, surface morphology, and film thickness (Igamov et al., 2926). Thermal treatment can modify

these features by promoting defect and/or particle reorganization and densification, surface restructuring, modification of thermally activated surface species, and the removal of weakly adhered or other undesirable features. These phenomena can affect optical absorption, apparent band-gap energy, and electrical transport, making annealing temperature a key processing parameter for determining the ultimate functionality of the films (Lin et al., 2013).

Doping provides an additional route for engineering the properties of TiO_2, and among the various elements investigated, Al is particularly attractive because it can influence the structural, optical, electrical, and surface properties of the host oxide. The observed effects depend strongly on dopant concentration, deposition method, substrate type, and thermal history. Bokov et al. (2021) investigated 0–5 mol% Al in TiO_2 films prepared by sol–gel-assisted spray pyrolysis at 500 °C. They reported decreases in grain size, interplanar spacing, surface roughness, and resistivity with increasing Al concentration, resulting in a minimum resistivity at 3 mol% and an increase in the optical band gap from approximately 3.28 to 3.39 eV.

In contrast, spin-coated Al-doped TiO_2 films developed as electron-transport layers for perovskite solar cells exhibited decreases in band-gap energy to 3.29, 3.25, and 3.18 eV at 1, 2, and 3% Al, respectively, compared with 3.38 eV for undoped TiO_2 (Moshfeghi and Entezari, 2022). Beldjebli et al. (2019) reported increased nanocrystallinity and grain size with Al addition in sol–gel dip-coated TiO_2 films, accompanied by a reduction in the band gap from 3.51 to 3.25 eV. Pulsed-laser-deposited Al-doped TiO_2 films have likewise shown concentration-dependent variations in optical and structural properties, with reported band-gap energies ranging from 3.43 to 3.61 eV (Abdulazeez and Salim, 2026). The deposition route is therefore an important consideration when comparing the properties of Al:TiO_2 films. Al-modified TiO_2 has been prepared using diverse techniques, including sol–gel processing, dip coating, spin coating, spray pyrolysis, pulsed-laser deposition, and atomic-layer deposition. These methods differ in precursor chemistry, growth mechanism, substrate-heating conditions, film thickness, and thermal history. Spray-pyrolysis studies have commonly examined the effects of controlled Al concentrations, whereas sol–gel approaches have investigated compositional changes in conjunction with post-deposition heat treatment (Mahu et al., 2021). Atomic-layer deposition, in particular, has been employed where controlled electrical conductivity and thermal stability are required. Consequently, the properties reported for these systems cannot be compared solely on the basis of nominal Al concentration because the films experience substantially different deposition and post-deposition histories.

For the present study, a nominal Al concentration of 2.0 mol% was selected and maintained throughout the experimental series. This concentration lies within the low-to-intermediate range investigated in previous studies of Al-doped TiO_2 (Afshar et al., 2016; Song et al., 2015). The choice was made to provide a fixed composition for assessing the independent influence of annealing temperature, rather than to identify 2.0 mol% as a universal optimum. Simultaneously varying the Al concentration and annealing temperature would introduce multiple variables, making it difficult to distinguish compositional effects from thermally induced changes. Maintaining a constant Al concentration therefore provides a controlled basis for evaluating the evolution of the optical, electrical, and morphological properties with temperature. Although previous studies have established the influence of Al incorporation and thermal treatment on TiO_2, much of the available literature has focused on varying the Al concentration under selected deposition or annealing conditions (Muaz et al., 2016). Consequently, the coupled evolution of optical, electrical, and surface characteristics under a systematic annealing-temperature series remains less clearly established for electrodeposited Al:TiO_2 films at a fixed Al concentration. A controlled experiment in which the dopant concentration and electrodeposition parameters remain unchanged while the annealing temperature is varied provides an opportunity to distinguish thermal effects from compositional effects. This is particularly relevant because optical transparency, electrical conductivity, and morphology may respond differently to thermal treatment.

Consequently, this study investigates electrodeposited Al:TiO_2 thin films prepared on indium tin oxide (ITO) substrates using identical deposition conditions. The nominal Al concentration was fixed at 0.2 mol%, while the annealing temperature was varied from 200 to 700 °C for 60 min. UV–visible spectroscopy was used to evaluate optical transmittance and apparent band-gap energy, electrical conductivity was measured using a four-point probe, and surface morphology was examined by scanning electron microscopy (SEM). Thus, annealing temperature was the principal experimental variable, while the Al concentration, precursor composition, substrate, deposition voltage, deposition duration, and other electrodeposition conditions were kept constant. The novelty of this work lies in the controlled correlation of the optical, electrical, and surface responses of electrodeposited Al:TiO_2 films across a systematic 200–700 °C annealing range at a fixed nominal Al concentration and under constant deposition conditions. Rather than claiming novelty from Al doping or annealing individually, the study establishes a processing–property relationship that clarifies how thermal treatment influences the apparent

band gap, optical transparency, electrical conductivity, and surface development of a compositionally controlled Al:TiO_2 system. The findings provide useful information for understanding and optimizing the thermal processing of Al:TiO_2 coatings for potential applications in optoelectronics, sensing, photo electrochemistry, and photovoltaics.

MATERIALS AND METHODS

Preparation of Al:TiO_2 Precursor

Aluminium-doped TiO_2 precursor solutions were prepared using titanium(IV) isopropoxide (TTIP) as the titanium precursor and aluminium nitrate nonahydrate [$Al(NO_3)_3 \cdot 9H_2O$] as the aluminium precursor. Isopropanol was used as the solvent, while acetylacetone served as a complexing agent for stabilizing the titanium precursor. A measured volume of 1.48 mL of TTIP was added dropwise to approximately 50 mL of isopropanol under continuous magnetic stirring. Acetylacetone was subsequently added at a 1:1 molar ratio relative to TTIP and stirring was continued to obtain a homogeneous precursor solution. A nominal Al/Ti molar ratio of 2.0 mol% was employed. Hence, 37.5 mg of $Al(NO_3)_3 \cdot 9H_2O$ was dissolved in a small volume of isopropanol and gradually added to the Ti-containing solution under continuous stirring. Additional isopropanol was then added to obtain a final precursor volume of 100 mL The resulting precursor solution was continuously stirred before electrodeposition. The precursor composition was maintained constant for all specimens, with annealing temperature serving as the principal experimental variable.

Substrate Preparation and Electrodeposition

The ITO-coated glass substrates were cleaned to remove surface contaminants that could adversely affect film adhesion and uniformity. The substrates were rinsed thoroughly with solvent, followed by rinsing with distilled/deionized water, and were subsequently dried before use. Electrodeposition was then carried out using a two-electrode configuration, with the ITO-coated glass substrate serving as the cathode and a carbon-graphite electrode serving as the counter electrode. Electrodeposition was performed using a two-electrode configuration in which the ITO-coated glass substrate served as the cathode and a carbon-graphite electrode served as the counter electrode. The electrodes were positioned parallel to each other with an inter-electrode separation of 30 mm. The precursor solution was continuously stirred during deposition to maintain solution homogeneity and facilitate mass transport. A constant cell voltage of 6.5 V was applied across the two electrodes, because the deposition system did not employ a reference electrode. The 6.5 V value represents the applied cell voltage rather than a controlled cathode potential relative to a reference electrode. The initial current was approximately 0.30 A and decreased progressively toward near-zero during deposition. The films were deposited for approximately 5 min under otherwise identical conditions. After deposition, the coated substrates were rinsed with distilled water to remove weakly adhered precursor residues and subsequently dried prior to annealing.

Thermal Annealing

The deposited films were annealed in air at 200, 300, 400, 500, 600, and 700 °C for 60 min. The annealing duration and other furnace conditions were maintained constant for all samples, while the annealing temperature was systematically varied. Following the 60-min thermal treatment, the furnace was switched off and the samples were allowed to cool naturally to room temperature inside the furnace. The samples remained in the furnace for approximately 24 h to ensure passive cooling to room temperature; this period did not represent an additional annealing or dwell time. This experimental arrangement enabled the effect of post-deposition annealing temperature to be investigated while maintaining a constant nominal precursor composition and deposition condition.

RESULTS AND DISCUSSION

Optical Transmittance

Figure 1 presents the UV–visible transmittance spectra of the Al_2 thin films annealed at temperatures ranging from 200 to 700 °C. All specimens exhibit relatively low transmission in the near-UV region, followed by a pronounced increase toward the visible region. The films maintain high optical transmission throughout the visible range, with transmittance values of approximately 91–93% between 450 and 800 nm. This behaviour indicates that the thermal treatment preserves the high visible-light transparency of the deposited Al_2 layers. A bare ITO substrate was used as the optical reference during the UV–visible measurements. Thus, the contribution of the ITO substrate to the reported transmittance spectra was accounted for by referencing the coated substrates against bare ITO. The spectra therefore primarily represent the optical response associated with the deposited Al_2 layer relative to the corresponding ITO substrate. This reference configuration was applied consistently to all samples to permit meaningful comparison of the temperature-dependent optical response. The position of the absorption edge varies with annealing temperature. With increasing temperature, the absorption edge shifts toward longer wavelengths, indicating a red shift in the optical absorption threshold. This behaviour is consistent with the reduction in apparent optical band-gap energy obtained from the Tauc analysis. The shift may reflect thermally induced changes in the electronic environment and microstructural organization of the

films. Previous studies have shown that annealing can produce different optical responses in TiO_2-based films depending on the material system and processing conditions, with reported changes in band gap associated with crystallization, nanostructural evolution, and defect-related effects (Kadri et al., 2021; Serafin et al., 2025). The small variations and intersections among the transmittance spectra in the visible region may result from differences in surface structure, refractive-index distribution, film thickness, and thin-film interference effects (Ballester et al., 2025). Because the present UV–visible and SEM measurements cannot independently resolve these contributions, the proposed mechanisms should be regarded as possible explanations rather than direct evidence of specific microscopic changes. However, the consistently high visible-light transmission demonstrates that the Al_2 films retain substantial optical transparency throughout the investigated annealing-temperature range.

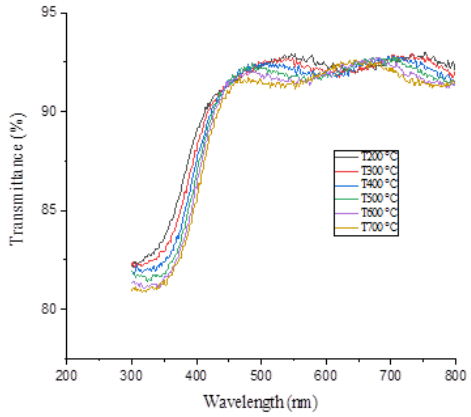


Figure 1: UV–visible transmittance spectra of Al:TiO_2 thin films annealed at different temperatures.

Apparent Optical Band Gap

The Tauc plots are presented in Figure 2, while Figure 3 illustrates the variation of the apparent optical band-gap energy with annealing temperature. The absorption coefficient, α, was calculated from the measured transmittance (T) using Eq. (1):

$$\alpha = \frac{1}{t} ln \frac{1}{T} \qquad (1)$$

where t represents the film thickness. The average film thickness was determined by the gravimetric method and was approximately 105 nm. The apparent optical band gap was subsequently estimated using the Tauc relation given in Eq. (2). For the present analysis, the films were treated using the direct allowed transition model, for which the Tauc relation is expressed as:

$$\alpha h\nu = A\left(h\nu - E_g\right)^{\frac{1}{2}} \qquad (2)$$

where $h\nu$ is the photon energy, A is a proportionality constant, and n depends on the nature of the electronic transition. For a direct allowed transition, $n = 2$, whereas $n = 1/2$, 2, and 2/3 correspond to indirect allowed, direct forbidden, and indirect forbidden transitions, respectively. The apparent band-gap energy was obtained by extrapolating the linear portion of the corresponding Tauc plot to $(\alpha h\nu)^2 = 0$. The apparent band-gap energy decreases progressively from approximately 3.00 eV at 200 °C to 2.85 eV at 700 °C, corresponding to a reduction of about 0.15 eV across the investigated temperature range. This decrease is accompanied by a displacement of the absorption edge toward longer wavelengths, indicating a measurable modification of the optical response following post-deposition thermal treatment. The observed variation may be associated with thermally induced changes in the electronic environment and microstructural organization of the films. Possible contributing factors include changes in local bonding, surface structure, particle development, crystallinity, lattice strain, and defect-related states.

However, these mechanisms cannot be distinguished using the present UV–visible and SEM measurements alone. In particular, the optical-transition characteristics of TiO_2 depend on its structural phase and degree of crystallinity. Anatase, rutile, and mixed-phase TiO_2 can exhibit different electronic structures and optical band-gap characteristics (Wang et al., 2025). Since X-ray diffraction was not performed in the present study, the crystalline phase and structural evolution of the films cannot be established directly. Similarly, since the chemical-state characterization was not performed, the possible contributions of specific defect states, oxygen-related defects, and changes in the chemical

environment associated with Al incorporation cannot be independently resolved from the present measurements (Mohd Said et al., 20218; Nowotny et al., 2015). Consequently, the observed 0.15 eV reduction should not be interpreted as direct evidence of a particular defect, phase transformation, or compositional mechanism. Although, the observed band-gap reduction is interpreted as an experimentally derived apparent optical band-gap evolution associated with thermal modification of the films' optical response, while the absence of XRD and chemical-state characterization precludes definitive attribution to a specific crystal phase, defect, lattice strain, or Al-related compositional mechanism, which would require complementary XRD and XPS analyses.

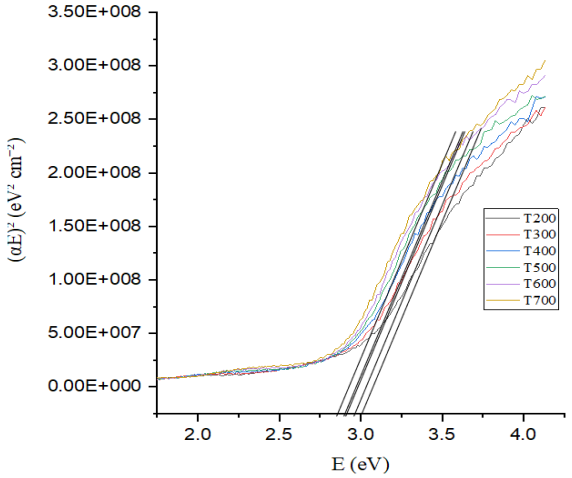


Figure 2: Tauc plots of Al:TiO_2 thin films annealed at different temperatures.

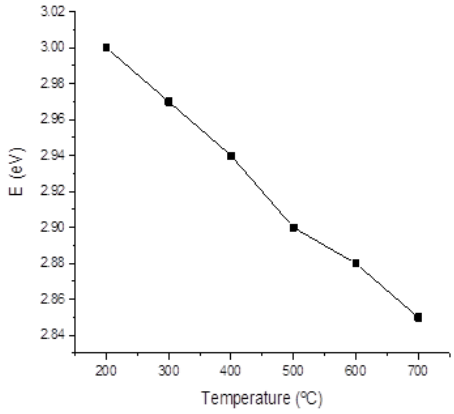


Figure 3: Variation of apparent optical band-gap energy of Al:TiO_2 thin films with annealing temperature.

Electrical Conductivity

The electrical characteristics of the Al:TiO_2 thin films were evaluated using a four-point-probe technique, and the measured parameters are summarized in Table 1. To distinguish the electrical response of the deposited Al:TiO_2 layer from that of the conductive ITO substrate, bare ITO substrates subjected to the corresponding thermal-treatment conditions were also evaluated. This control measurement provides a direct basis for assessing whether the temperature-dependent electrical response observed for the Al:TiO_2/ITO structures can be attributed primarily to changes in the deposited film.

For the Al:TiO_2-coated samples, the measured conductivity increased progressively from 1.263 S cm^{-1} at 200 °C to 3.609 S cm^{-1} at 700 °C. For the same temperature range, sheet resistance decreases from 7.917×10^4 to 2.771×10^4 Ω, while resistivity decreases from 0.792 to 0.277 Ω cm. The reciprocal relationship between conductivity and resistivity is maintained throughout the dataset, confirming the consistency of the calculated electrical parameters using Eq. (3), (4), and (5).

$$R_s = \frac{\pi}{\ln(2)}\frac{\Delta V}{I} \quad (3)$$

$$\rho_s = R_s\, t \quad (4)$$

$$\sigma_s = \frac{1}{\rho_s} \quad (5)$$

Where t is the thickness of the film and $\pi/\ln 2 = 4.532$. The conductivity enhancement is consistent with improved electrical connectivity within the film. A possible explanation is that annealing modifies the physical arrangement and interparticle contact within the deposited layer. The increase in the electrical response with annealing temperature may be associated with thermally induced changes in the physical organization of the deposited layer. Annealing can promote particle rearrangement, densification, and improved interparticle contact, thereby reducing discontinuities and facilitating more continuous charge-transport pathways (Maisungnoen et al., 2026).

The SEM observations provide qualitative morphological information consistent with such an interpretation. However, the observed conductivity enhancement cannot be attributed exclusively to changes in crystallinity, defect concentration, carrier concentration, or carrier mobility because these parameters were not directly measured in the present study. This caution is warranted because thermal treatment can simultaneously modify the structural and electronic characteristics that govern charge transport in TiO_2-based films (Chen et al., 2017; Kanmaz and Tomakin, 2024). Since the nominal Al concentration and deposition conditions were maintained constant, the systematic variation in conductivity is associated

principally with the change in annealing temperature within the experimental design. The highest measured conductivity of 3.609 S cm^{-1} and the lowest calculated resistivity of 0.277 Ω cm were obtained after annealing at 700 °C. Within the investigated temperature range, this condition therefore produced the strongest measured electrical response. This observation should not be interpreted as a universal optimum, because the appropriate thermal treatment depends on the simultaneous optical, morphological, structural, and electrical requirements of the intended application.

Table 1: Electrical parameters of Al:TiO_2 thin films annealed at different temperatures

Temperature (°C)	Sheet Voltage (V)	Sheet Current (A)	Sheet Resistance (Ω)	Sheet Resistivity (Ω cm)	Sheet Conductivity (S cm^{-1})
200	1.52E-02	1.92E-07	7.917E+04	0.792	1.263
300	1.49E-02	2.17E-07	6.866E+04	0.687	1.456
400	1.53E-02	2.36E-07	6.483E+04	0.648	1.542
500	1.51E-02	2.80E-07	5.393E+04	0.539	1.854
600	1.50E-02	3.41E-07	4.399E+04	0.440	2.273
700	1.51E-02	5.45E-07	2.771E+04	0.277	3.609

Surface Morphology

The surface morphology of the Al_2 films annealed at 200–700 °C is shown in Figure 4. Noticeable changes in surface texture and particle arrangement occur across the annealing-temperature range. The film annealed at 200 °C exhibits relatively small surface features separated by discernible interparticle regions and localized voids. At 300 and 400 °C, the surface features become more pronounced, suggesting progressive thermal modification of the as-deposited film structure. A further change is observed at 500 °C, where the surface appears comparatively compact, with several regions showing closer particle-to-particle contact. At 600 and 700 °C, the microstructure becomes less uniform, accompanied by variations in the apparent feature dimensions and spacing between adjacent particles. These observations suggest that thermal treatment promotes rearrangement of the deposited material and modifies the spatial organization of the film surface (Divya et al., 2020). The morphological evolution shows qualitative correspondence with the electrical behaviour. The apparently closer particle contact at higher annealing temperatures may reduce discontinuities within the deposited layer and facilitate charge transport. This interpretation is consistent with the progressive increase in measured conductivity across the annealing series. However, the SEM observations alone cannot establish the specific microscopic mechanism responsible for the electrical enhancement (Asalzadeh and Yasserian, 2019).

The SEM analysis is therefore interpreted primarily as qualitative evidence of temperature-dependent surface evolution. The micrographs demonstrate changes in surface appearance and particle organization but do not, by themselves, permit reliable determination of crystallite size, quantitative porosity, pore-size distribution, crystal structure, lattice strain, or defect concentration. Quantitative image analysis combined with XRD and chemical-state characterization would be required to establish these parameters more rigorously.

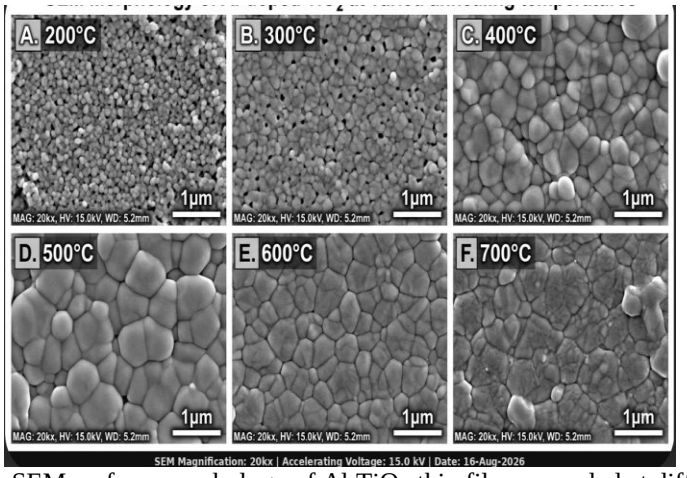


Figure 4: SEM surface morphology of Al:TiO_2 thin films annealed at different temperatures.

Correlation between Optical, Electrical, and Surface Morphological Properties

The combined optical, electrical, and morphological results demonstrate a systematic dependence of the Al_2 films on annealing temperature. The apparent optical band gap decreases from 3.00 eV at 200 °C to 2.85 eV at 700 °C, while the measured electrical conductivity increases from 1.263 to 3.609 S cm^{-1}. The simultaneous changes indicate that post-deposition thermal treatment modifies both the optical absorption response and the measured electrical transport characteristics of the deposited film. The SEM observations provide complementary evidence of temperature-dependent changes in particle development, interparticle spacing, and surface organization. The progressive increase in measured conductivity may therefore be associated, at least qualitatively, with improved physical connectivity within the deposited layer. Improved interparticle contact can provide more continuous transport pathways, while changes in surface organization may reduce discontinuities and interfacial resistance (Rettenmaier et al., 2019; Ajayi et al., 2021). Nevertheless, the present characterization does not permit the conductivity enhancement to be uniquely attributed to crystallinity, defect concentration, carrier density, carrier mobility, or any specific microscopic transport mechanism. The optical response exhibits a concurrent decrease in apparent band-gap energy and red shift of the absorption edge with increasing annealing temperature. This trend demonstrates a measurable thermal modification of the optical response but does not by itself establish whether the change originates from crystallization, phase transformation, strain relaxation, defect-related states, Al incorporation, or another structural or electronic effect. Such attribution would require complementary structural and chemical-state measurements.

An important feature of the present results is that high visible-light transmission is retained while the measured electrical response increases across the annealing-temperature series. The 700 °C specimen exhibits the highest measured conductivity while maintaining the generally high visible-light transmission observed for the film series. This combination may be relevant to applications requiring simultaneous optical transparency and electrical transport (Ajayi et al., 2025). However, the present measurements demonstrate a processing–property relationship rather than direct device functionality. Photovoltaic and photoelectrochemical applications would require dedicated measurements of parameters such as open-circuit voltage, short-circuit current density, fill factor, and power-conversion efficiency [21]. Similarly, sensing and photocatalytic applications require application-specific performance evaluations. Moreover, the results demonstrate that controlled post-deposition annealing provides an effective means of modifying the optical, electrical, and surface characteristics of electrodeposited Al_2 films prepared at a fixed nominal Al concentration. The systematic temperature series enables the thermal contribution to the measured film properties to be examined without simultaneously changing the dopant concentration or electrodeposition conditions

CONCLUSION

Al:TiO_2 thin films were successfully electrodeposited on ITO substrates at a fixed nominal Al concentration and subsequently annealed from 200 to 700 °C for 60 min. Increasing the annealing temperature produced systematic changes in the measured optical, electrical, and surface properties. The films maintained high visible transmittance, reaching approximately 91–93% over 450–800 nm, while the apparent optical band gap decreased from 3.00 to 2.85 eV. In parallel, electrical conductivity increased from 1.263 to 3.609 S cm^{-1}, accompanied by a reduction in resistivity from 0.792 to 0.277 Ω cm. SEM observations showed temperature-dependent changes in surface organization and interparticle connectivity that may contribute to the observed conductivity enhancement, although the microscopic transport mechanism cannot be established from the present measurements alone. The overall results demonstrate that annealing temperature is an effective processing parameter for modifying the functional properties of electrodeposited Al_2 films at constant nominal Al concentration. The 700 °C film exhibited the highest measured conductivity while retaining high visible transmittance among the investigated conditions. However, the observed trends should not be interpreted as defining a universal optimum, and further structural and chemical characterization, particularly XRD and XPS, is required to clarify the origins of the thermal response.

Recommendations

Future studies should employ X-ray diffraction to determine the crystalline phase, crystallite size, lattice parameters, strain, and structural evolution of the Al:TiO_2 films with annealing temperature. X-ray photoelectron spectroscopy would further assist in verifying Al incorporation and examining the chemical states of Ti, O, and Al. Quantitative measurements of film thickness, surface roughness, particle-size distribution, and surface porosity should also be undertaken to strengthen the relationship between thermal treatment and film architecture. Repeated electrical measurements should be used to establish measurement uncertainty, while Hall-effect characterization, where available, would provide information on carrier concentration and mobility. For application-oriented development, the annealed films should be incorporated into suitable device structures

and evaluated using application-specific performance parameters. For photovoltaic or photoelectrochemical applications, measurements of open-circuit voltage, short-circuit current density, fill factor, and power-conversion efficiency under controlled illumination are recommended. Such investigations would establish whether the favourable material properties observed in the present study translate into measurable device performance.

REFERENCES

Abdulazez, A. A., & Salim, K. D. (2026). Characterization of aluminum-doped titanium dioxide thin films prepared by pulsed-laser deposition. *Iraqi Journal of Applied Physics, 22*(1), 19–23. doi:10.2025/jhqzjm55

Afshar, S., Pordel, S., Tahmouresilerd, B., & Azad, A. (2016). Improving the photocatalytic activity of modified anatase TiO_2 with different concentrations of aluminum under visible light: Mechanistic survey. *Photochemistry and Photobiology, 92*(6), 783–789. doi:10.1111/php.12665

Ajayi, A. A., Alabi, A. B., Abodunrin, O. W., & Musiliyu, K. A. (2021). Structural and optical characterization of chemically synthesized nanostructured zinc oxide thin film. *ABUAD International Journal of Natural and Applied Sciences, 1*(1), 18–23. doi:10.53982/aijnas.2021.0101.03-j

Ajayi, A. A., Alabi, A. B., Salau, A. O., Ogunmola, E. D., Akinsola, S. I., Abodunrin, O. W., Oluyemi, F. O., Olawole, O. C., Musiliyu, K. A., & Abejide, F. H. (2025). Effect of annealing temperature on the properties of Cu_2ZnSnS_4 (CZTS) thin films for solar cell application. *Jordan Journal of Physics, 18*(4), 477–488. doi:10.47011/18.4.6

Asalzadeh, S., & Yasserian, K. (2019). The effect of various annealing cooling rates on electrical and morphological properties of TiO_2 thin films. *Semiconductors, 53*(12), 1603–1607. doi:10.1134/S1063782619160036

Ballester, M., Marquez, E., Bass, J., Würsch, C., Willomitzer, F., & Katsaggelos, A. K. (2025). Review and novel formulae for transmittance and reflectance of wedged thin films on absorbing substrates. *Measurement Science and Technology, 36*(2), 025502. doi:10.1088/1361-6501/ada305

Beldjebli, O., Bensaha, R., Ocak, Y. S., Amirache, L., & Boukherroub, R. (2019). Synthesis and photocatalytic efficiency of sol-gel Al^{3+}-doped TiO_2 thin films: Correlation between the structural, morphological and optical properties. *Materials Research Express, 6*(8), 085036.

Bokov, D., Turki Jalil, A., Chupradit, S., Suksatan, W., Javed Ansari, M., Shewael, I. H., Valiev, G. H., & Kianfar, E. (2021). Nanomaterial by sol-gel method: Synthesis and application. *Advances in Materials Science and Engineering, 2021*, Article 5102014. doi:10.1155/2021/5102014 [Retracted in 2025]

Chen, J., Tao, H. B., & Liu, B. (2017). Unraveling the intrinsic structures that influence the transport of charges in TiO_2 electrodes. *Advanced Energy Materials, 7*(23), 1700886. doi:10.1002/aenm.201700886

Divya, P., Arulkumar, S., Parthiban, S., Goswami, A., Ahamad, T., & Gawande, M. B. (2020). Rapid and scalable wire-bar strategy for coating of TiO_2 thin-films: Effect of post-annealing temperatures on structures and catalytic dye-degradation. *Molecules, 25*(7), 1683. doi:10.3390/molecules25071683

Igamov, B. D., Bekpulatov, I. R., Normamatov, A. M., Kamardin, A. I., Kodirova, F. S., & Imanova, G. (2026). Comprehensive analysis of thickness-dependent structural, morphological, and optical properties of TiO_2-based thin films. *Results in Optics, 23*, 100993. doi:10.1016/j.rio.2026.100993

Kadri, L., Bulai, G., Carlescu, A., George, S., Gurlui, S., Leontie, L., Doroftei, C., & Adnane, M. (2021). Effect of target sintering temperature on the morphological and optical properties of pulsed laser deposited TiO_2 thin films. *Coatings, 11*(5), 561. doi:10.3390/coatings11050561

Kalinina, E., & Pikalova, E. (2021). Opportunities, challenges and prospects for electrodeposition of thin-film functional layers in solid oxide fuel cell technology. *Materials, 14*(19), 5584. doi:10.3390/ma14195584

Kanmaz, İ., & Tomakin, M. (2024). Improving solar cell efficiency through controlled annealing effects of TiO_2 thin films. *Physica Status Solidi A, 221*(5), 2300647. doi:10.1002/pssa.202300647

Kumar, S. A., Sahoo, S., Laxminarayana, G. K., & Rout, C. S. (2024). Electrochemical deposition for cultivating nano- and microstructured electroactive materials for supercapacitors: Recent developments and future perspectives. *Small, 20*(40), 2402087. doi:10.1002/smll.202402087

Lin, C. P., Chen, H., Nakaruk, A., Koshy, P., & Sorrell, C. C. (2013). Effect of annealing temperature on the photocatalytic activity of TiO_2 thin films. *Energy*

Procedia, *34*, 627–636. doi:10.1016/j.egypro.2013.06.794

Liu, S., Tian, J., & Zhang, W. (2021). Fabrication and application of nanoporous anodic aluminum oxide: A review. *Nanotechnology*, *32*(22), 222001. doi:10.1088/1361-6528/abe25f

Mahu, E., Coromelci, C. G., Lutic, D., Asaftei, I. V., Sacarescu, L., Harabagiu, V., & Ignat, M. (2021). Tailoring mesoporous titania features by ultrasound-assisted sol-gel technique: Effect of surfactant/titania precursor weight ratio. *Nanomaterials*, *11*(5), 1263.doi:10.3390/nano11051263

Mohd Said, N. D., Sahdan, M. Z., Nayan, N., Saim, H., Adriyanto, F., Bakri, A. S., & Morsin, M. (2018). Difference in structural and chemical properties of sol-gel spin coated Al doped TiO_2, Y doped TiO_2 and Gd doped TiO_2 based on trivalent dopants. *RSC Advances*, *8*, 29686–29697. doi:10.1039/C8RA03950J

Moshfeghi, E., & Entezari, M. H. (2022). Enhancement of the photovoltaic performance of perovskite solar cells via sono-synthesis of Al-doped TiO_2 as the electron transport layer. *International Journal of Energy Research*, *46*(15), 23465–23479. doi:10.1002/er.8643

Muaz, A. K. M., Hashim, U., Ibrahim, F., Thong, K. L., Mohktar, M. S., & Liu, W. W. (2016). Effect of annealing temperatures on the morphology, optical and electrical properties of TiO_2 thin films synthesized by the sol-gel method and deposited on Al/TiO_2/SiO_2/p-Si. *Microsystem Technologies*, *22*(4), 871–881. doi:10.1007/s00542-015-2514-7

Musiliyu, K. A., Ogunmola, E. D., Ajayi, A. A., & Abodunrin, O. W. (2023). Effect of concentration on the properties of nitrogen-doped zinc oxide thin films grown by electrodeposition. *Materials for Renewable and Sustainable Energy*, *12*, 23–29. doi:10.1007/s40243-022-00225-0

Nowotny, J., Alim, M. A., Bak, T., Idris, M. A., Ionescu, M., Prince, K., & Sigmund, W. (2015). Defect chemistry and defect engineering of TiO_2-based semiconductors for solar energy conversion. *Chemical Society Reviews*, *44*(23), 8424–8442. doi:10.1039/C4CS00469H.

Rettenmaier, K., Zickler, G. A., Redhammer, G. J., Anta, J. A., & Berger, T. (2019). Particle consolidation and electron transport in anatase TiO_2 nanocrystal films. *ACS Applied Materials & Interfaces*, *11*(43), 39859–39874. doi:10.1021/acsami.9b12693

Serafin, J., Bujaldón, R., Sreńscek-Nazzal, J., Kałamaga, A., Gomez, E., Vendrell, X., & Serra, A. (2025). Transition metal-doped TiO_2 and CeO_2 photocatalysts modified with Ti_3C_2 MXene for PMS-driven advanced oxidation of pharmaceutical pollutants. *Chemical Engineering Journal*, *524*, 169005. doi:10.1016/j.cej.2025.169005

Song, Y. S., Kim, B. Y., Cho, N. I., & Lee, D. Y. (2015). Effect of Al doping on optical band gap energy of Al–TiO_2 thin films. *Journal of Nanoscience and Nanotechnology*, *15*(7), 5228–5231. doi:10.1166/jnn.2015.10380

Sun, Y., Li, C., Liu, D., Zhang, F., Xue, J., & Zheng, Q. (2025). Surface and interfacial engineering for multifunctional nanocarbon materials. *ACS Nano*, *19*(2), 1944–1980. https://doi.org/10.1021/acsnano.4c14128